Available online at www.sciencedirect.com
SCIENCE DIRECT
ELSEVIER
International Journal of Mass Spectrometry 249–250 (2006) 420–425
International Journal of Mass Spectrometry
www.elsevier.com/locate/ijms

Mass spectrum of the 1-butene-3-yne-2-yl radical (i-C_4H_3; X^2A')

Ying Guo, Xibin Gu, Ralf I. Kaiser*

Department of Chemistry, University of Hawai'i at Manoa, Honolulu, HI 96822, USA

Received 11 October 2005; received in revised form 16 November 2005; accepted 16 November 2005
Available online 27 December 2005

Abstract

The crossed molecular beams method has been applied to produce the 1-butene-3-yne-2-yl radical, i-$C_4H_3(X^2A')$ under single collision conditions via the reaction of dicarbon molecules with ethylene. We recorded time-of-flight spectra of the radical at the center-of-mass angle (28.0°) of the parent ion ($m/z = 51$; $C_4H_3^+$) and of the fragments at $m/z = 50$ ($C_4H_2^+$), $m/z = 49$ (C_4H^+), $m/z = 48$ (C_4^+), $m/z = 39$ ($C_3H_3^+$), $m/z = 38$ ($C_3H_2^+$), $m/z = 37$ (C_3H^+), and $m/z = 36$ (C_3^+). This yielded relative intensity ratios of $I(m/z = 51):I(m/z = 50):I(m/z = 49):I(m/z = 48):I(m/z = 39):I(m/z = 38):I(m/z = 37):I(m/z = 36) = 0.47 \pm 0.01:0.94 \pm 0.01:1.0:0.07 \pm 0.02:0.31 \pm 0.01:0.23 \pm 0.02:0.24 \pm 0.01:0.12 \pm 0.01$ at 70 eV electron impact energy. Upper limits at mass-to-charge ratios between 27 and $m/z = 24$ and $m/z = 14$–12 were derived to be 0.02 ± 0.01. Note that the intensity of the ^{13}C isotopic peak of the 1-butene-3-yne-2-yl radical at $m/z = 52$ ($^{13}C^{12}C_3H_3^+$) is about 0.04 ± 0.01 relative to $m/z = 51$. Employing linear scaling methods, the absolute electron impact ionization cross section of the 1-butene-3-yne-2-yl radical was computed to be $7.8 \pm 1.6 \times 10^{-16}$ cm^2. These data can be employed to monitor the 1-butene-3-yne-2-yl radical in oxygen-poor combustion flames and in the framework of prospective explorations of planetary atmospheres (Jupiter, Saturn, Uranus, Neptune, Pluto) and of their moons (Titan, Triton, Oberon) in situ via matrix interval arithmetic assisted mass spectrometry.

Keywords: Electron impact ionization; Fragmentation pattern; Mass spectrum; Free radical

1. Introduction

Free hydrocarbon radicals are central reactive intermediates in astrochemistry [1], planetary atmospheres [2,3], and in combustion flames [4–6]. Resonantly stabilized free radicals (RSFR) such as the C_{2v} symmetric propargyl (C_3H_3) or the 1-butene-3-yne-2-yl (i-C_4H_3; H_2CCCCH; C_s point group) radicals are of particular importance. Both open shell species are believed to play a crucial role in the formation of polycyclic aromatic hydrocarbons (PAHs) and soot in the combustion of fuels [7–34]. In RSFRs, the unpaired electron is delocalized and spread out over two or more sites in the molecule. This results in a number of resonant electronic structures of comparable importance. Due to the delocalization, resonantly stabilized free hydrocarbon radicals are more stable than ordinary radicals, have lower enthalpies of formation, and normally form weaker bonds with stable molecules (including molecular oxygen) [35–37]. These weakly bound addition complexes are not easily stabilized by collisions at high temperature. Consequently, RSFRs are relatively unreactive and can reach high concentration in flames. These high concentrations and the relatively fast rates of the radical–radical reactions make them important intermediates to form complex hydrocarbons in flames. Therefore, both in the terrestrial settings like combustion flames [38] and extraterrestrial environments such as the interstellar medium [39] and planetary atmospheres [40–42], these radicals and the i-C_4H_3 isomer in particular have been suggested as precursors to complex polycyclic aromatic hydrocarbons and possibly fullerenes like C_{60} [43]. Nevertheless, despite the importance of the i-C_4H_3 radical in combustion processes and in the chemical processing of hydrocarbon rich planetary atmospheres, the mass spectrum of this molecule is still obscure [44]. However, a detailed knowledge of the fragmentation pattern will help to follow combustion flames in real time and to determine absolute radical concentrations not only via spectroscopic techniques (Fourier transform microwave spectroscopy [45]; laser induced fluorescence [46]), but also via mass spectrometry coupled to an electron impact ionizer. Very recently, a powerful combination of quadrupole mass spectrometry (QMS) with matrix interval arithmetic (MIA) has been shown to be capable of extracting the chemical composition

* Corresponding author. Tel.: +1 808 9565730; fax: +1 808 9565908.
E-mail address: kaiser@gold.chem.hawaii.edu (R.I. Kaiser).

1387-3806/$ – see front matter © 2005 Elsevier B.V. All rights reserved.
doi:10.1016/j.ijms.2005.11.013

of complex gas mixtures on line and in situ even in the presence of thermally labile molecules [47]. To extend this method to radicals, the fragmentation patterns of these molecules such as of the *i*-C_4H_3 radical are crucial. For example, signal at $m/z = 51$ from $C_4H_3^+$ – the parent ion of the *i*-C_4H_3 radical – can be contaminated from the fragmentation of more complex hydrocarbons such as butatriene (C_4H_4) and benzene (C_6H_6). Therefore, the ion current recorded at $m/z = 51$ presents actually the sum of the ion currents of all molecules contributing to this mass-to-charge ratio. We would like to stress that in principle, selective photoionization utilizing a tunable ultraviolet photon source – a soft ionization technique which effectively eliminates the fragmentation of the radical cation to smaller fragments – coupled to a mass spectrometric device is feasible to reveal the time dependent concentrations of radials in combustion flames [48]. However, since this technique requires a tunable vacuum ultraviolet light source – either a synchrotron or four wave mixing schemes – this method can hardly be utilized to identify radicals in the framework of an in situ exploration of hydrocarbon-rich atmospheres of planets and their moons via space crafts.

In this paper, we present the first mass spectrum of the 1-butene-3-yne-2-yl radical, *i*-$C_4H_3(X^2A')$, which is prepared in situ under single collision conditions in a crossed molecular beams experiment [49]. In contrast to bulk experiments, where reactants are mixed, the key benefit of a crossed beams method is the capability to form both reactants, here dicarbon molecules and ethylene, in separate supersonic beams. The reactants of each beam are made to collide only with the molecules of the other beam, and the products formed fly undisturbed towards the mass spectrometric detector. These features provide an unparalleled method to scrutinize the outcome of a single collision event and also to *synthesize* unstable radicals such as *i*-$C_4H_3(X^2A')$ excluding higher order collisions.

2. Experimental setup

We generated the 1-butene-3-yne-2-yl radical (*i*-C_4H_3; X^2A') in a crossed molecular beams reaction of the dicarbon molecule, $C_2(X^1\Sigma_g^+/a^3\Pi_u)$, with ethylene, C_2H_4, in situ. Briefly, the main chamber of the crossed beams machine is pumped to the low 10^{-8} Torr region. Two source chambers – each pumped by a 2000 l s^{-1} and a 430 l s^{-1} maglev pump – are located inside the vessel (Fig. 1). A pulsed supersonic beam of dicarbon molecules, $C_2(X^1\Sigma_g^+/a^3\Pi_u)$, was generated via laser ablation of graphite at 266 nm [50]. Here, the 30 Hz, 10 mJ output of a Spectra Physics GCR-270-30 Nd:YAG laser is focused onto a rotating carbon rod. Ablated dicarbon molecules are seeded into helium carrier gas released by a Proch-Trickl pulsed valve operating at 60 Hz and 80 μs pulses with 4 atm backing pressure. A four slot chopper wheel located between the skimmer and a cold shield selects a segment of the seeded dicarbon carbon beam with a peak velocity of 1969 ± 2 m s^{-1} and a speed ratio S of 5.5 ± 0.1. The pulsed dicarbon and the pulsed ethylene beam (550 Torr backing pressure; $v_p = 890 \pm 5$ m s^{-1}; $S = 15.7 \pm 0.1$) pass through skimmers and cross at 90° in the interaction region of the scattering chamber. The time-of-flight spectra of the parent

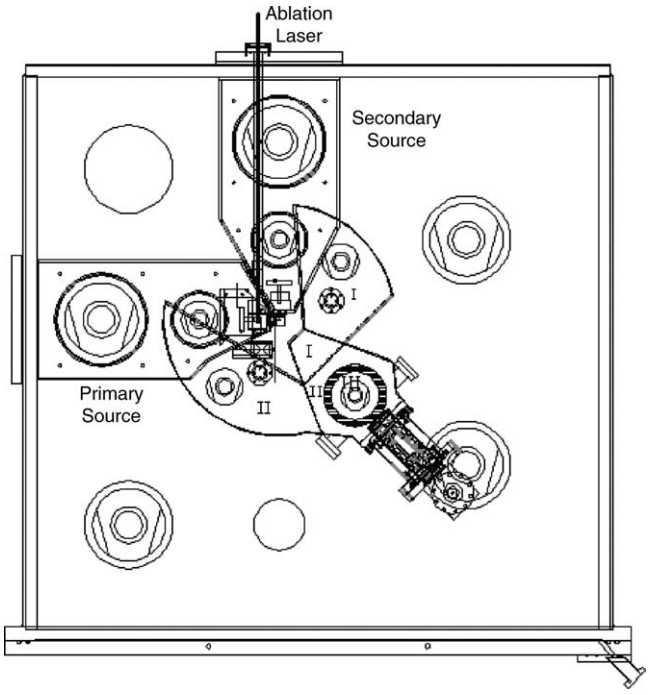

Fig. 1. Top view of crossed molecular beams machine and the detector system.

and of the fragmentation patterns of the newly formed *i*-C_4H_3 radical were recorded in the plane of both beams using a rotatable quadrupole mass spectrometer with an electron-impact ionizer at the center-of-mass angle of the reaction of 28.0°. The Brink-type electron impact ionizer [51] is surrounded by a liquid nitrogen shield and is located in the third region of a triply differentially pumped ultra high vacuum chamber (10^{-11} Torr) (Fig. 1); the quadrupole mass filter and the Daly-type scintillation particle detector [52] are connected to the second region. Note that the fragmentation patterns of a molecule strongly depend on the kinetic energy of the electron. Here, we recorded these patterns at 70 eV electron energy, i.e., the *standardized* electron energy utilized to setup the NIST mass spectral database.

3. Results

The experimental strategy is similar to the one utilized previously in our laboratory to extract the mass spectrum of the linear butadiynyl radical, $C_4H(X^2\Sigma^+)$ [53]. Firstly, we have to account for the fact that the ablation beam does not contain solely the dicarbon molecule but also carbon atoms, $C(^3P_j)$, and the tricarbon molecule, $C_3(X^1\Sigma_g^+)$ [50]. The presence of the tricarbon molecules does not obstruct the reactive scattering signal since the reaction with ethylene was found to occur only at collision energies higher than 41 ± 1 kJ mol^{-1} [54]. In the present experiment, the collision energies were determined to be 30.2 kJ mol^{-1} (dicarbon-ethylene) and 36.8 kJ mol^{-1} (tricarbon-ethylene). However, we have to point out that bimolecular collisions of ground state carbon atoms with ethylene are very rapid within gas kinetics and were found to form the propargyl radical plus atomic hydrogen via reaction (1) in a strongly exoergic reaction [55]. On the other

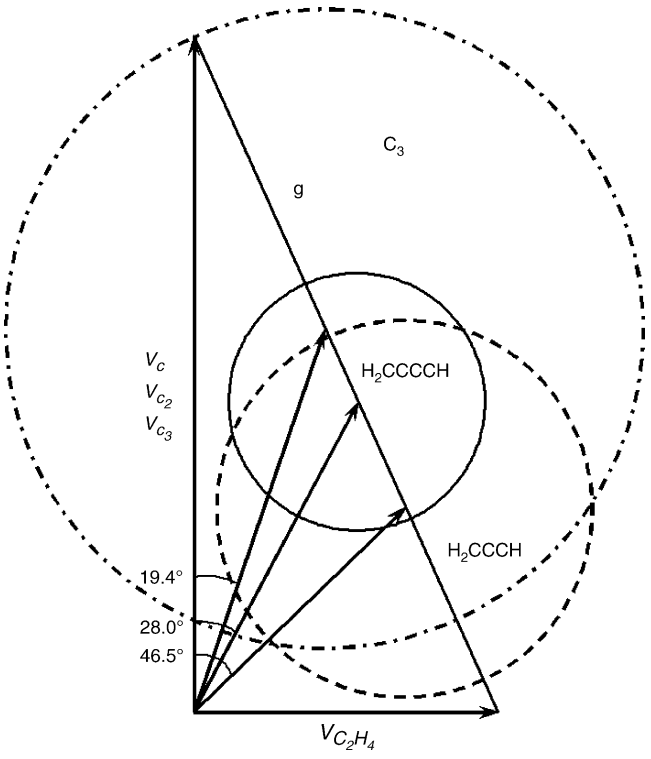

Fig. 2. Newton diagram of the reactions of carbon atoms and dicarbon molecules with ethylene via Eqs. (1) and (2). The maximum recoil velocities of the propargyl (C_3H_3), the 1-butene-3-yne-2-yl radical (i-C_4H_3), and C_3 (inelastically scattering with ethylene) are shown as dashed, solid, and dashed–dotted circles. See text for a detailed definition of the symbols.

hand, reactions of dicarbon with ethylene synthesize solely the 1-butene-3-yne-2-yl radical, i-C_4H_3 (reaction (2)) [56]:

$$C(^3P_j) + C_2H_4 \rightarrow H_2CCCH + H \quad (1)$$

$$C_2(X^1\Sigma_g^+/a^3\Pi_u) + C_2H_4 \rightarrow i\text{-}C_4H_3 + H. \quad (2)$$

Secondly, we have to find a method to distinguish if the reactive scattering signal actually comes from the reaction of carbon atoms or from dicarbon molecules with ethylene. Considering the mass of the i-C_4H_3 radical of 51 amu, we expect that signal at $m/z = 51$ and of the fragmentation patterns at 50 ($C_4H_2^+$), 49 (C_4H^+), and 48 (C_4^+) comes solely from the i-C_4H_3 radical. Conversely, ions at lower mass-to-charge ratios of 39 ($C_3H_3^+$), 38 ($C_3H_2^+$), and 37 (C_3H^+) originate either from the fragmentation of the i-C_4H_3 radical in the electron impact ionizer or from the propargyl radical (reaction (1)) and its fragmentation patterns. Note that signal at $m/z = 36$ (C_3^+) has contributions from reactions (1) and (2) as well as from inelastically scattered tricarbon molecules from the ethylene beam. It is imperative distinguish these pathways. Here, we performed a transformation of the coordinate system from the laboratory system to the center-of-mass reference frame. The latter is convenient to get information on the dynamics of reactions (1) and (2). Recall that the experimentalist 'sits' on the center-of-mass and watches: (i) how the dicarbon collides with the ethylene molecule and (ii) in which direction the i-C_4H_3 radical and the hydrogen atom – as well as the propargyl radical product – leave. Fig. 2 compiles the relationship between both coordinate systems and incorporates the dynamics of the reactions (1) and (2).

In the present experiment, a beam of the dicarbon with a lab velocity V_{C_2} crosses a supersonic beam of ethylene with a lab velocity $V_{C_2H_4}$ at 90° (Fig. 2). These velocities are represented as vectors. The vector connecting the tips of the dicarbon and ethylene vectors defines the relative velocity vector $\boldsymbol{g}$. Note that in the laboratory system, the center of mass frame moves with the velocity $\boldsymbol{V}_{CM}$. With respect to the dicarbon beam, this vector holds a fixed center-of-mass angle, Θ_{CM}, of 28.0° and 46.5° for the reactions of ethylene with dicarbon and atomic carbon, respectively. The center-of-mass velocity vector starts at the crossing point of the reactant beams and terminates at the center-of-mass of the system which is actually located on the relative velocity vector $\boldsymbol{g}$. Since we have two reactions – those of ethylene with dicarbon and atomic carbon – concurrently, we also have to label two center-of masses, $CM_{C_2H_4/C_2}$ and $CM_{C_2H_4/C}$, which are both located on the relative velocity vector $\boldsymbol{g}$ (Fig. 2). These center-of-masses play a key role to distinguish if the signal at lower mass-to-charge-ratios actually originates from reaction (1) and (2) alone or a combination of both pathways.

To set apart both options, we can investigate the energetics of reactions (1) and (2) in depth. The total, maximum available energy, $E_{available}$, of each reaction, which can be released in translational energy of the reaction products, is simply the sum of the collision energy, E_c, plus the absolute of the exoergicity of the reaction, $\Delta_R G^\circ$, i.e., 215 ± 8 and 160 ± 5 kJ mol^{-1} for reactions (1) and (2), respectively. Energy and momentum conservation dictates how the available energy will be partitioned among the reaction products; this enables us to compute the maximum recoil velocities of the heavy reaction products of H_2CCCH (reaction (1)) and i-C_4H_3 (reaction (2)) in the center-of-mass system ($u_{C_3H_3}$ and $u_{C_4H_3}$);

$$u_{C_3H_3} = \sqrt{\frac{2m_H E_{available}}{m_{C_3H_3}(m_{C_3H_3} + m_H)}} \quad (3)$$

$$u_{C_4H_3} = \sqrt{\frac{2m_H E_{available}}{m_{C_4H_3}(m_{C_4H_3} + m_H)}} \quad (4)$$

Principally, these product molecules can scatter in a sphere which is centered at the center-of-mass of the reaction; this sphere holds a *radius* of a velocity vector. If we project these spheres into the two-dimensional velocity vector diagram (Fig. 2) around the center-of-mass of the reaction yields two circles with *radii* of $u_{C_3H_3}$ (dashed circle) and $u_{C_4H_3}$ (solid circle).

A thorough examination of these recoil circles, the so called *Newton Circles*, presents essential guidance for the crossed beams experiment and for the elucidation of the mass spectrum of the 1-butene-3-yne-2-yl radical. Let us track a line from the crossing point of the supersonic dicarbon and the ethylene beams along the center of mass of the velocity vector of the dicarbon plus ethylene reaction – placed 28.0° relative to the dicarbon vector – to the center-of-mass of the reaction. This vector crosses first the Newton circle of the propargyl radical reaction product (reaction (1)) and then the Newton circle of the

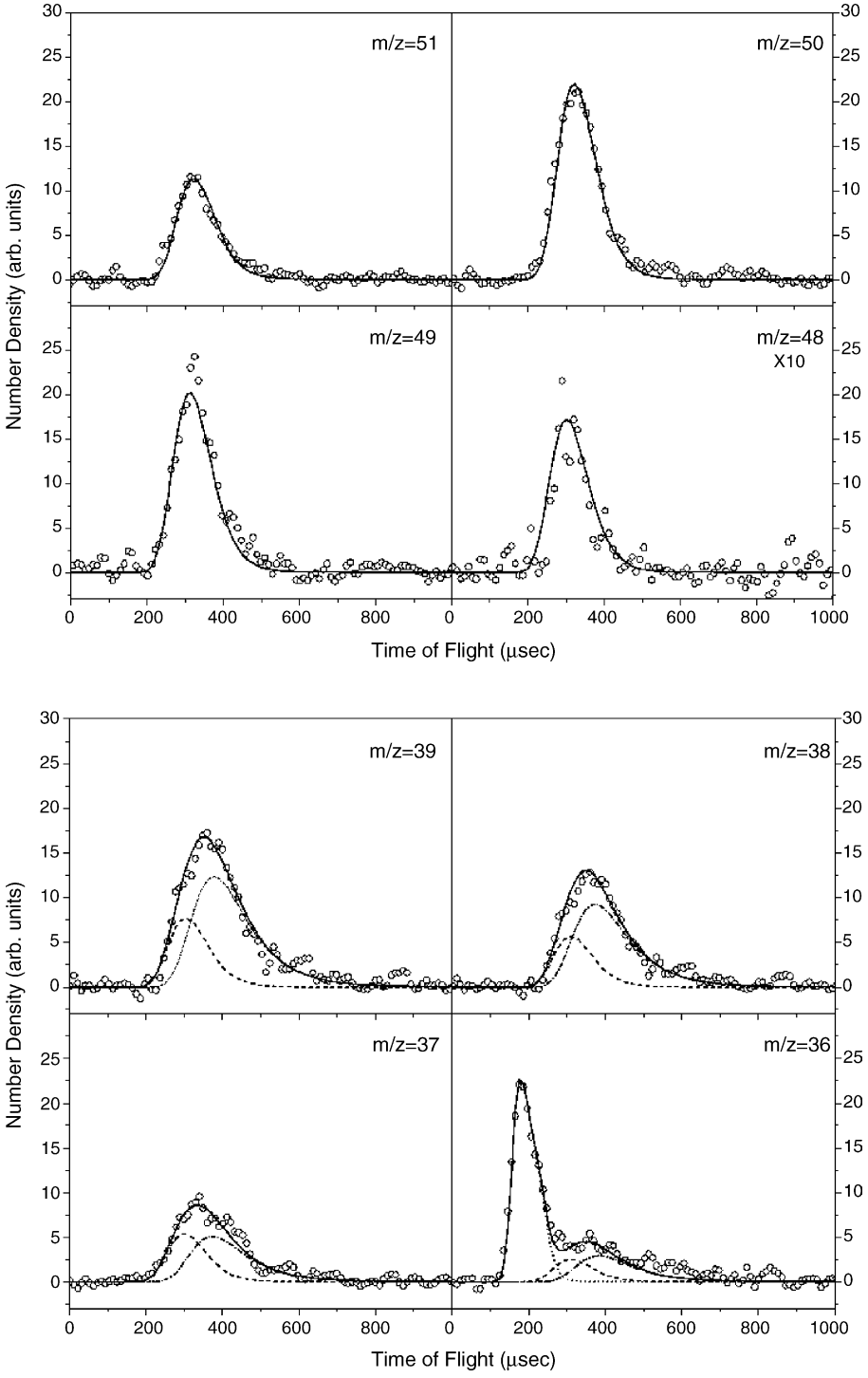

Fig. 3. Time-of-flight spectra of the 1-butene-3-yne-2-yl radical and its fragmentation pattern at various mass-to-charge ratios. The circles represent the experimental data, the lines the fits derived from the dynamics of the carbon-ethylene (dash–dot line), dicarbon-ethylene (dashed line) and tricarbon-ethylene (dot line) systems. Data were taken with a mass resolution of 1 amu.

i-C_4H_3 radical (reaction (2)). This suggests that TOF spectra recorded at m/z values of 39 and lower will have contributions from two channels, i.e., from the propargyl radical and it fragmentation patterns and also from the fragments of the *i*-C_4H_3 radical. Most important, the center-of-mass velocity vector crosses also the Newton Circle of inelastically scattered tricarbon molecules; therefore, signal at $m/z = 36$ has also a third component coming from inelastically scattered tricarbon molecules (Figs. 2 and 3). Selected time-of-flight spectra recorded at the center-of-mass angle of 28.0° are shown in Fig. 3. Here, the time-of-flight spectra taken at $m/z = 51$–48 are – after scaling – super imposable and could be fit with identical center-of-mass functions derived from reaction (2) [53]. This supports the deduction from Fig. 2 that ions at these

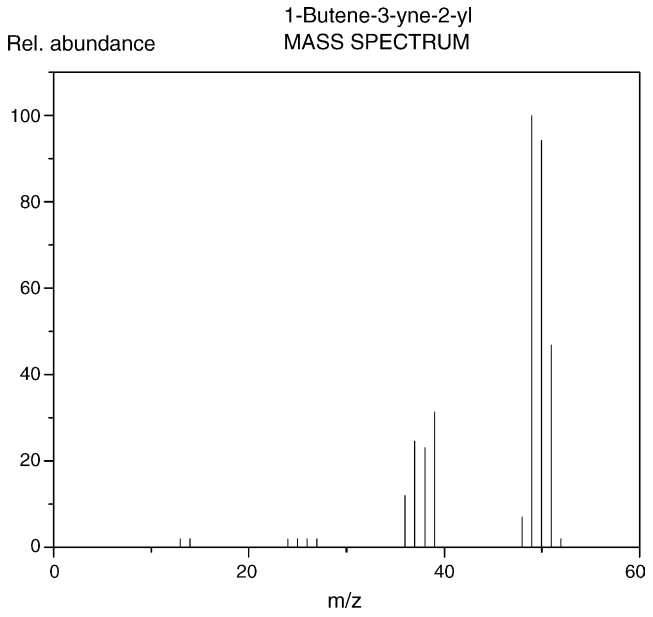

Fig. 4. Mass spectrum of the 1-butene-3-yne-2-yl radical synthesized from the recorded parent peak and fragmentation pattern; the spectrum is presented in a NIST standardized format.

masses come from the $C_4H_3^+$ parent and from its fragment down to C_4^+. It is evident that the time-of-flight spectra at $m/z = 39$–37 have two contributions: a slower part from reaction (1) and a faster part from reaction (2). Consequently, the latter presents the contribution of the fragmentation pattern of the $C_4H_3^+$ parent to $m/z = 39$–37. Finally, signal at $m/z = 36$ must be fit with three channels, i.e., from reactions (1) and (2) as well as inelastically scattered tricarbon molecules (Fig. 2). By integrating these time-of-flight spectra and normalizing them to the most intense peak, this yielded relative intensity ratios of $I(m/z = 51):I(m/z = 50):I(m/z = 49):I(m/z = 48):I(m/z = 39):I(m/z = 38):I(m/z = 37):I(m/z = 36) = 0.47 \pm 0.01:0.94 \pm 0.01:1.0:0.07 \pm 0.02:0.31 \pm 0.01:0.23 \pm 0.02:0.24 \pm 0.01:0.12 \pm 0.01$ at 70 eV electron impact energy. Upper limits at mass-to-charge ratios between 27 and $m/z = 24$ and $m/z = 14$–12 were derived to be 0.02 ± 0.01. Note that the intensity of the ^{13}C isotopic peak of the 1-butene-3-yne-2-yl radical at $m/z = 52$ ($^{13}C^{12}C_3H_3^+$) is about 0.04 ± 0.01 relative to $m/z = 51$. The synthesized mass spectrum of the 1-butene-3-yne-2-yl radical is shown in Fig. 4.

To quantify the concentrations of the 1-butene-3-yne-2-yl radical in hydrocarbon flames and in planetary atmospheres, we would like to approximate the absolute, total ionization cross section of the *i*-C_4H_3 radical at 70 eV electron energy. Recall that in the range of 70–80 eV, the total electron impact ionization cross section, σ_{ion}, is – within ±20% – proportional to the averaged molecular polarizibility, α [57]. The authors approximated the molecular polarizibility via the sum of the atomic polarizibilities. Taking the atomic polarizibilities of carbon and hydrogen as 1.76×10^{-24} and 0.6668×10^{-24} cm^3 [58], we can calculate the ratio of the cross section of ethylene to the *i*-C_4H_3 radical to 0.69 ± 0.14. Note that ethylene has been used as a reference molecule because the structure of the ethylene molecule (carbon–carbon double bond) and the *i*-C_4H_3 radical are similar; since the absolute electron impact ionization cross section of the ethylene molecule is known to be 5.39×10^{-16} cm^2 at 70 eV [59], we can estimate the total, absolute ionization cross section of the *i*-C_4H_3 radical to be $7.8 \pm 1.6 \times 10^{-16}$ cm^2.

4. Conclusions

The crossed molecular beams method was exploited to form the 1-butene-3-yne-2-yl radical, *i*-$C_4H_3(X^2A')$ under single collision conditions via the reaction of dicarbon molecules with ethylene. Time-of-flight spectra of the radical were recorded at the center-of-mass angle of 28.0° at mass-to-charge ratios of $m/z = 51$ ($C_4H_3^+$; parent ion) and of the fragments at $m/z = 50$–48 and $m/z = 39$–36. Integrating these time-of-flight spectra and normalizing them to the most intense peak, intensity ratios of $I(m/z = 51):I(m/z = 50):I(m/z = 49):I(m/z = 48):I(m/z = 39):I(m/z = 38):I(m/z=37):I(m/z = 36) = 0.47 \pm 0.01:0.94 \pm 0.01:1.0:0.07 \pm 0.02:0.31 \pm 0.01:0.23 \pm 0.02:0.24 \pm 0.01:0.12 \pm 0.01$ at 70 eV electron impact energy can be extracted. Upper limits at mass-to-charge ratios between 27 and $m/z = 24$ and $m/z = 14$–12 were derived to be 0.02 ± 0.01. Note that the intensity of the ^{13}C isotopic peak of the 1-butene-3-yne-2-yl radical at $m/z = 52$ ($^{13}C^{12}C_3H_3^+$) is about 0.04 ± 0.01 relative to $m/z = 51$. In addition, the absolute ionization cross section of the butadiynyl radical has been determined to be $7.8 \pm 1.6 \times 10^{-16}$ cm^2. These data can be utilized in future space missions to detect the *i*-C_4H_3 radical – a crucial reaction intermediates in the formation of polycyclic aromatic hydrocarbon molecules – in the atmospheres of hydrocarbon rich planets (Jupiter, Saturn, Uranus, Neptune, Pluto) and their moons (Titan) and also in combustion flames via mass spectrometry coupled with matrix interval arithmetic. The reader should keep in mind that the actual fragmentation patterns also depend on the internal energy of the neutral radical to be ionized. An investigation of the ratio of the fragmentation pattern of, for instance, $m/z = 51$ and 50 depicts a very mild fluctuation of less than 5% over a collision energy range of 12–51 kJ mol^{-1}. This error could be included into the matrix interval arithmetic.

Acknowledgements

This work was supported by the National Science Foundation (CHE-0234461; YG, RIK) and by the US Department of Energy-Basic Energy Sciences (DE-FG02-03ER15411; XG, RIK).

References

[1] Y.C. Minh, E.F. van Dishoeck, Astrochemistry: From Molecular Clouds to Planetary Systems, Astronomical Society of the Pacific, San Francisco, 2000.
[2] M.V. Sykes, The Future of Solar System Exploration, Astronomical Society of the Pacific, San Francisco, 2002.
[3] M.E. Summers, D.F. Strobel, APJ 346 (1989) 495.
[4] J.H. Kiefer, S.S. Sidhu, R.D. Kern, K. Xie, H. Chen, L.B. Harding, Combust. Sci. Technol. 82 (1992) 101.
[5] M. Hausmann, K.H. Homann, Proceedings of 22nd International Annual Conference of ICT, (Combust. React. Kinetics), 1991, p. 1.
[6] H.Y. Zhang, J.T. McKinnon, Combust. Sci. Technol. 107 (1995) 261.
[7] A. D'anna, A. Violi, A. D'allessio, Combust. Flame 121 (2000) 418.

[8] A. D'anna, A. Violi, Proc. Combust. Inst. 27 (1998) 425.
[9] T. Faravelli, A. Goldaniga, E. Ranzi, Proc. Combust. Inst. 27 (1998) 1489.
[10] J. Appel, H. Bockhorn, M. Frenklach, Combust. Flame 121 (2000) 122.
[11] H. Wang, M. Frenklach, Combust. Flame 110 (1997) 173.
[12] R.P. Lindstedt, G. Skevis, Proc. Combust. Inst. 26 (1996) 703.
[13] P. Lindstedt, Proc. Combust. Inst. 27 (1998) 269.
[14] P. Dagaut, M. Cathonnet, Combust. Flame 113 (1998) 620.
[15] P.R. Westmoreland, A.M. Dean, J.B. Howard, J.P. Longwell, J. Phys. Chem. 93 (1989) 8171.
[16] A. Lamprecht, B. Atakan, K. Kohse-Höinghaus, Combust. Flame 122 (2000) 483.
[17] F. Hartlieb, B. Atakan, K. Kohse-Höinghaus, Combust. Flame 121 (2000) 610.
[18] B. Atakan, A.T. Hartlieb, J. Brand, V. Kohse-Höinghaus, Proc. Combust. Inst. 27 (1998) 435.
[19] C. Douté, J.-L. Delfau, C. Vovelle, Combust. Sci. Technol. 103 (1994) 153.
[20] C.J. Pope, J.A. Miller, Proc. Combust. Inst. 28 (2000) 1579.
[21] M.J. Castaldi, N.M. Marinov, C.F. Melius, J. Hwang, S.M. Senkan, W.J. Pitz, C.K. Westbrook, Proc. Combust. Inst. 26 (1996) 693.
[22] N.M. Marinov, W.J. Pitz, C.K. Westbrook, M.J. Castaldi, S.M. Senkan, Combust. Sci. Technol. 116/117 (1996) 211.
[23] C.F. Melius, M.E. Colvin, N.M. Marinov, W.J. Pitz, S.M. Senkan, Proc. Combust. Inst. 26 (1996) 685.
[24] J.A. Miller, J.V. Volponi, J.-F. Pauwels, Combust. Flame 105 (1996) 451.
[25] J-F. Pauwels, J.V. Volponi, J.A. Miller, Combust. Sci. Technol. 110/111 (1995) 249.
[26] J.A. Miller, C.F. Melius, Combust. Flame 91 (1992) 21.
[27] C.F. Melius, J.A. Miller, E.M. Evleth, Proc. Combust. Inst. 24 (1992) 621.
[28] S.G. Davis, C.K. Law, H. Wang, Proc. Combust. Inst. 27 (1998) 305.
[29] S.E. Stein, J.A. Walker, M. Suryan, A. Fahr, Proc. Combust. Inst. 23 (1990) 85.
[30] J.A. Miller, Proc. Combust. Inst. 20 (1984) 461.
[31] H. Richter, J.B. Howard, Prog. Energy Combust. Sci. 26 (2000) 565.
[32] S.E. Wheeler, W.D. Allen, H.F. Schaefer III, J. Chem. Phys. 121 (2004) 8800.
[33] S.J. Klippenstein, J.A. Miller, J. Phys. Chem. A 109 (2005) 4285.
[34] X. Krokidis, N.W. Moriarty, W.A. Lester Jr., M. Frenklach, Int. J. Chem. Kinet. 33 (2001) 808.
[35] D.B. Atkinson, J.W. Hudgens, J. Phys. Chem. A 103 (1999) 4242.
[36] D.K. Hahn, S.J. Klippenstein, J.A. Miller, Faraday Discuss. 119 (2001) 79.
[37] I.R. Slagle, D. Gutman, Proc. Combust. Inst. 21 (1986) 875.
[38] M. Hausmann, P. Hebgen, K.H. Homann, Proceedings of the 24th Symposium (International) on Combustion, 1992, p. 793.
[39] D. Teyssier, D. Fosse, M. Gerin, P. Maryvonne, A. Abergel, E. Habart, Proceedings of the Conference, Waterloo, ON, Canada, August 21–23, 2002, 2003, pp. 422–424.
[40] F. Stahl, P.v.R.F. Schleyer, H.F. Schaefer, R.I. Kaiser, Planet. Space Sci. 50 (2002) 685.
[41] L.M. Lara, R.R. Rodrigo, A. Coustenis, J.J. Lopez-Moreno, E. Chassefiere, European Space Agency, Special Publication SP-338, 1991, p. 137.
[42] G. Gladstone, M. Allen, Y.L. Yung, Icarus 119 (1996) 1.
[43] G.S. Hammond, V.J. Kuck, Fullerenes, American Chemical Society, Washington, DC, 1992.
[44] http://webbook.nist.gov/chemistry/.
[45] M. Nakajima, Y. Sumiyoshi, Y. Endo, Rev. Sci. Instrum. 73 (2002) 165.
[46] K. Hoshina, K. Kennosuke, Y. Ohshima, Y. Endo, J. Chem. Phys. 108 (1998) 108.
[47] R.I. Kaiser, P. Jansen, K. Petersen, K. Roessler, Rev. Sci. Instrum. 66 (1995) 5226.
[48] C.Y. Ng, Vacuum Ultraviolet Photoionization and Photodissociation of Molecules and Clusters, World Scientific, Singapore, 1991.
[49] R.I. Kaiser, Chem. Rev. 102 (2002) 1309;
A.F. Furlan, G.E. Hall, J. Chem. Phys. 109 (1998) 10390;
A. Furlan, J. Phys. Chem. B 103 (1999) 1550;
X. Yang, K. Liu, Modern Trends in Chemical Dynamics, World Scientific, Singapore, 2003;
R.A. Dressler, Chemical Dynamics in Extreme Environments, World Scientific, Singapore, 2001.
[50] R.I. Kaiser, A.G. Suits, Rev. Sci. Instrum. 66 (1995) 5405.
[51] G.O. Brink, Rev. Sci. Instrum. 37 (1966) 857, other IJMS paper.
[52] N.R. Daly, Rev. Sci. Instrum. 31 (1960) 264.
[53] X. Gu, Y. Guo, R.I. Kaiser, Int. J. Mass Spectrom. 246 (2005) 29.
[54] R.I. Kaiser, T.N. Le, T.L. Nguyen, A. Mebel, N. Balucani, Y.T. Lee, F. Stahl, P.v.R. Schleyer, H.F. Schaefer III, Faraday Discuss. 119 (2001) 51.
[55] R.I. Kaiser, Y.T. Lee, A.G. Suits, J. Chem. Phys. 105 (1996) 8705.
[56] N. Balucani, A.M. Mebel, Y.T. Lee, R.I. Kaiser, J. Phys. Chem. A 105 (2001) 9813.
[57] R.L. Summers, Empirical observations of the sensitivity of hot cathode ionization type vacuum gauges, NASA Technical Note TN D-5285, 1969;
R. Holanda, Sensitivity of hot cathode ionization vacuum gauges in several gases, NASA Technical Note TN D-6815, 1972.
[58] CRC Handbook of Chemistry and Physics, National Institute of Standards, Boca Raton, 2004.
[59] C. Tian, C.R. Vidal, Chem. Phys. Lett. 288 (1998) 499;
C. Tian, C.R. Vidal, J. Phys. B 31 (1998) 895.